Article

Not peer-reviewed version

Soil erosion and landslide susceptibility mapping using Rock Engineering System methodology: The case of Mandra fatal flash flood (2017) in Western Attica, Greece

Nikolaos Tavoularis *

Posted Date: 11 October 2023

doi: 10.20944/preprints202308.0978.v2

Keywords: mandra flash flood; soil erosion; slope failure; RES; mitigation measures; landslide susceptibility

Article

Soil Erosion and Landslide Susceptibility Mapping Using Rock Engineering System Methodology: The Case of Mandra Fatal Flash Flood (2017) in Western Attica, Greece

Nikolaos Tavoularis [1] *

[1] Dr. Engineering Geologist of National Technical University of Athens Regional Authority of Attica / Directorate of Technical Works, Department of Technical Support of Attica's Region Municipal Islands, 185 45, Greece; ntavoularis@patt.gov.gr

* Correspondence: ntavoularis@metal.ntua.gr.

Abstract: Two of the eight main soil degradation processes to which soils worldwide are confronted, are soil erosion and landslides. Specifically, landslides are a major threat in particular areas across Europe, often leading to serious impacts on population, property, and infrastructure. Regarding the above-mentioned, a case study from the Mandra fatal flash flood (happened on 14-15 November 2017) in the Attica Region (Greece), is presented with the intention of assessing the relationship between the soil erosion and the landslide incidents. Investigations have been executed from 2018 until 2022, and the outcomes of those have been taken under consideration by the Technical Authority of the Attica Region. Soil erosion lines have been delineated in GIS and have been validated by an already generated regional Web-GIS landslide susceptibility map. The study presents soil erosion types from Mandra fatal flash flood event and correlates them with the already existing landslide susceptibility analysis for Attica Region. The produced susceptibility map is a cartographic product in a regional scale (1:100,000) generated via a semi-quantitative heuristic methodology named Rock Engineering System (RES). The way this landslide susceptibility map is generated, can be the basis for proposing modeling approaches that can respond to new developments in the European landslide policies.

Keywords: mandra flash flood; soil erosion; slope failure; RES; mitigation measures; landslide susceptibility

1. Introduction

Soil erosion is a crucial triggering factor of land degradation worldwide and specifically at the European level, with serious financial implications. To this end, the European Commission's Thematic Strategy for Soil Protection recognizes soil erosion as a serious threat to the European Union's (EU) soil resources [1]. Focusing more on soil erosion types, soil erosion by water as well as gully erosion are two typical causes of land degradation that lead subsequently to slope failures. For those reasons, different stakeholders need easy access to soil data and information of various types and scales to assess the state of soils [2]. Many researchers so far, have used a variety of qualitative and quantitative techniques with erosion models, integrating GIS applications to cope with soil erosion and land degradation issues [3]. To be more specific, soil erosion prediction models have been used to predict the hazard of soil erosion [4,5]. In addition, the most common erosion model is the Universal Soil Loss Equation (USLE) and its revised version (RUSLE), which estimates long-term average annual soil loss [6–8]. Considering spatial distribution, USLE/RUSLE models have limitations, which have been dealt with using geospatial applications [9]. On the other hand, soil erosion assessment in large-scale field measurements may cause some drawbacks as being time-consuming, expensive, or nearly impossible due to limited resources [10,11]. In addition to this, soil erosion assessment models as such RUSLE/USLE have some drawbacks when predicting sediment pathways from hill slopes to water bodies and gully assessment [12].

Preprints (www.preprints.org) | NOT PEER-REVIEWED | Posted: 11 October 2023 doi:10.20944/preprints202308.0978.v2

Moreover, regarding gully erosion which is a major land degradation process and probably the most severe type of water erosion (and this type of erosion appears to occur very often in the broader study area of Mandra city), gully erosion susceptibility mapping is a valuable tool, as it is beneficial for identifying the spatial probability of gully incidents.

Traditional statistical models have been implemented to estimate gully erosion susceptibility mapping, such as analytical hierarchical process (AHP) [13], frequency ratio (FR) [14], logistic regression (LR) [15], and weight of evidence [16], where the prediction accuracy is relatively low by using those methods [17–19]. However, the gully erosion susceptibility mapping prediction accuracy has been greatly improved using machine learning algorithms compared with traditional statistical models [20,21]. Particularly, different machine learning algorithms have been used for gully erosion [22–25].

On the other hand, the application of machine learning algorithms in gully susceptibility mapping in large areas using very high-resolution datasets, has also limitations regarding computing efficiency (e.g., a pixel-by-pixel prediction is needed). In such a case, the spatial resolution must be reduced in order to improve the above-mentioned computing efficiency. As a result, this procedure may reduce prediction accuracy [26]. In Table 1, a summary of the above-described methodologies is presented.

Table 1. Some characteristics methodologies for the assessment of different types of soil erosion.

Methodologies for the assessment of different types of soil erosion	Researchers	Number of References
Universal Soil Erosion Equation (USLE)	Wischmeier and Smith (1978), Panagos et al. (2015)	[6], [8]
Revised USLE	Renard et al. (1997), Panagos et al. (2015)	[7], [8]
Frequency Ratio (FR)	Conforti et al., 2011	[14]
Logistic Regression (LR)	Conoscenti et al., 2014	[15]
Analytical Hierarchical process (AHP)	Arabameri et al., 2018	[13]
Weight of Evidence (WoE)	Arabameri et al., 2019	[16]
Machine Learning algorithms	Eustace et al., 2011; Rahmati et al., 2017); Arabameri et al., 2019; Pourghasemi et al., 2017	[22], [23], [16], [25]

Thus, to predict soil erosion types (gully included) with high accuracy, especially in areas where severe phenomena (extremely heavy rainfall, such as the one happened in Mandra on 14-15 November 2017) may occur, a more practical methodology still needs to be invented.

In this context, as land degradation (e.g., landslides) is associated to soil erosion, it is believed that finding tools and methodologies to cope with slope failures, automatically somebody succeed in addressing issues caused by soil erosion. This statement is strengthened by the fact that researchers have obtained more reliable soil erosion susceptibility outcomes by using slope failure events and soil erosion conditioning factors have been used in landslide susceptibility prediction [27]. For example, researchers found a correlation between landslide manifestation and soil erosion in several locations [28].

Based on the high intensity of the Mandra fatal flash (with short duration) flood event of 14-15 November 2017, the erosivity of rainfall and run-off were (among other parameters) the main causes for loosening the soil (and the weathering mantle of decomposed – fragmented rocks), resulting in weakening the slopes and as a result leading to mass movements of solid and semi-solid materials [29,30].

In addition, fires which have manifested in the broader area of Mandra recently, can be a catalyst for erosion and landslides [31]. Thus, the consequences of fires, the fact that in the broader area of Mandra, a not properly urban expansion has taken place in the last 40 years, as well as the triggering

 doi:10.20944/preprints202308.0978.v2

factor of heavy rainfall of 14-15 November 2017, have intensified the extension of gullies (soil erosion) and landslides. Another characteristic point that relates landslides to soil erosion and particularly gullies in the study area, is due to slope modifications during human interference [e.g., cut and fill or artificial drains) [32,33].

In the paper of Rozos et al. [28], it is mentioned that many studies correlate slope failure phenomena with soil erosion processes. In their research, data referring to many landslides along the study area permitted the evaluation of their map based on the RUSLE model.

Besides, Lee et al. [34], verified erosion map against landslide locations using the Geographic Information System (GIS). In this research, a determination of soil erosion potential was validated using the actual location of slope failures.

Pradhan et al. [35], studied an area, constructing a landslide map that was used to validate soil erosion intensity. In their research, it was mentioned that the spatial assessment of soil erosion was needed, because this phenomenon was the main cause of land sliding in the study area. To justify their scope of this research, they claimed that the control of soil erosion became essential to preventing landslides.

Yuan-jun et al. [36], Lian et al. [37], Swanson and Dyrness [38], and Wang et al. [39], mention that landslides have been frequently reported due to soil erosion in China, because of an increase in mining activities and agricultural production. Also, Shen et al. [40], and Wu et al. [41] refer to failures of shallow slopes due to soil erosion observed in this China.

Acharya et al. [42], refer to rainfall events on steep hillslopes that cause both soil erosion and shallow landslides which in turn interact with each other. They investigated that soil erosion in landslide areas is significantly more serious. They mention that generally, there is a satisfactory correspondence between landslides and soil erosion, but a quantitative study on the association between these two variables on a large representative scale is still lacking.

Lin et al. [43], studied changes of the post-earthquake landslides and vegetation recovery conditions and assessed soil loss using multi-temporal SPOT images, an NDVI- based vegetation recovery index and a Universal Soil Loss Equation (USLE). They concluded that assessment of soil erosion at landslides is an important task for decision-making and policy planning in studied landslide area.

Belayneh et al. [44], refer to the fact that gullies and landslides often share common environmental controls and can interact with each other, even though the triggering conditions of the two processes are often different. It is also mentioned that the number of gully densities within and outside the slope failures were compared in order to judge the interaction between gullies and landslides. They also add that their research, regarding large regions, is one of the very few that definitely depicts the role of slope failures as a process resulting in the occurrence of gullies [45–47].

Huang et al. [48], claimed that soil erosion provides slide mass sources for landslide formation and studied the influence of the soil material source on landslide evolution. Therefore, it was possible to obtain more reliable landslide susceptibility prediction results by introducing soil erosion as a geology and hydrology-related predisposing factor. Their results indicated that soil erosion factor plays the most important role in landslide susceptibility prediction among all the selected predisposing factors.

Finally, Kou et al. [49], revealed a satisfactory linear fitting result between the area of landslides and soil erosion. They concluded, that restoring vegetation cover in landslide scars should become the most urgent action to mitigate soil erosion.

Regarding the examined area, two characteristic types of slope failures have been recorded: (i) earth falls and (ii) rock falls according to Varnes classification [50], whereas in the broader area of Attica Region, there are, furthermore: debris fall, earth slump, earth slide, rockslide-debris avalanche, taking into consideration Varnes classification [50]. Analysis of those slope failures has been developed by Tavoularis et al. [51].

Based on the above-mentioned, a case study from the Mandra fatal flash flood (which took place on 14-15 November 2017) in the Attica Region (Greece), is presented with the intention to explore the role of soil erosion in relation to land degradation (e.g., landslides). Investigations from different

 doi:10.20944/preprints202308.0978.v2

stakeholders have been executed from 2018 until 2022, and the outcomes of those have been taken under consideration by the Technical Authority (Directorate of Technical Works) of Attica Region to design and implement a priori mitigations measures (for debris flows and rainfall-induced soil erosion processes) against potential upcoming extreme rainfall episodes. Through a variety of tools, soil erosion types are defined and delineated in GIS maps and afterwards validated by an already generated regional Web-GIS landslide susceptibility map of the Attica Region (DIAS project) which was fulfilled in June of 2021 by a research team [51], implementing a semi-quantitative methodology named Rock Engineering System (RES). This map identifies specific zoning areas which are more susceptible to slope failure. The way this landslide susceptibility map is generated, can be the basis for modeling approaches that can respond to new developments in European policies (e.g., data, maps, technical reports) such as those of the European landslide susceptibility map version 2 [(ELSUS v2) and ELSUSv2_six_datasets & metadata] [52] or more over to the improvement of large-scale assessments, which can further generate landslide hazard and risk maps. Thus, the objective of this study is to explore the relation of soil erosion to landsliding using methodologies that have been implemented in landslide susceptibility modelling. As per the author's best of knowledge, no one else has predicted (at least at the Greek and European levels) the soil erosion susceptibility using a semi-quantitative methodology such as RES. Thus, implementing methodologies that have already been used in landslide susceptibility mapping, this can help identify and estimate soil erosion hazards. The current article is organized as follows: a brief description of the fatal flash flood that happened in Mandra (November of 2017) is firstly presented. Then, the soil erosion types that took place in that examined area are described. In addition, landslide susceptibility analysis for the Attica Region via a semi-quantitative heuristic methodology named Rock Engineering System (RES) is also shortly analyzed. The outcomes (e.g., inventory and landslide susceptibility map) of using this methodology are depicted to validate the correlation between landslide occurrences and soil erosion events manifested in Mandra area. Moreover, some characteristic mitigation measures that have been designed are addressed against potential upcoming new extreme rainfall episodes. The paper is finally concluded with suggestions for future research.

2. Materials and Methods

2.1. Location of the study area

The study concerns the area upstream of the residential area of Mandra and extends from the ridge of the adjacent mountain range (Pateras Mountain) with an altitude of 841m to the settlement of Mandra (Figure 1). The study area covers the catchment areas of the two streams Agia Aikaterini and Soures located upstream of the settlement of Mandra.

Preprints (www.preprints.org) | NOT PEER-REVIEWED | Posted: 11 October 2023 doi:10.20944/preprints202308.0978.v2

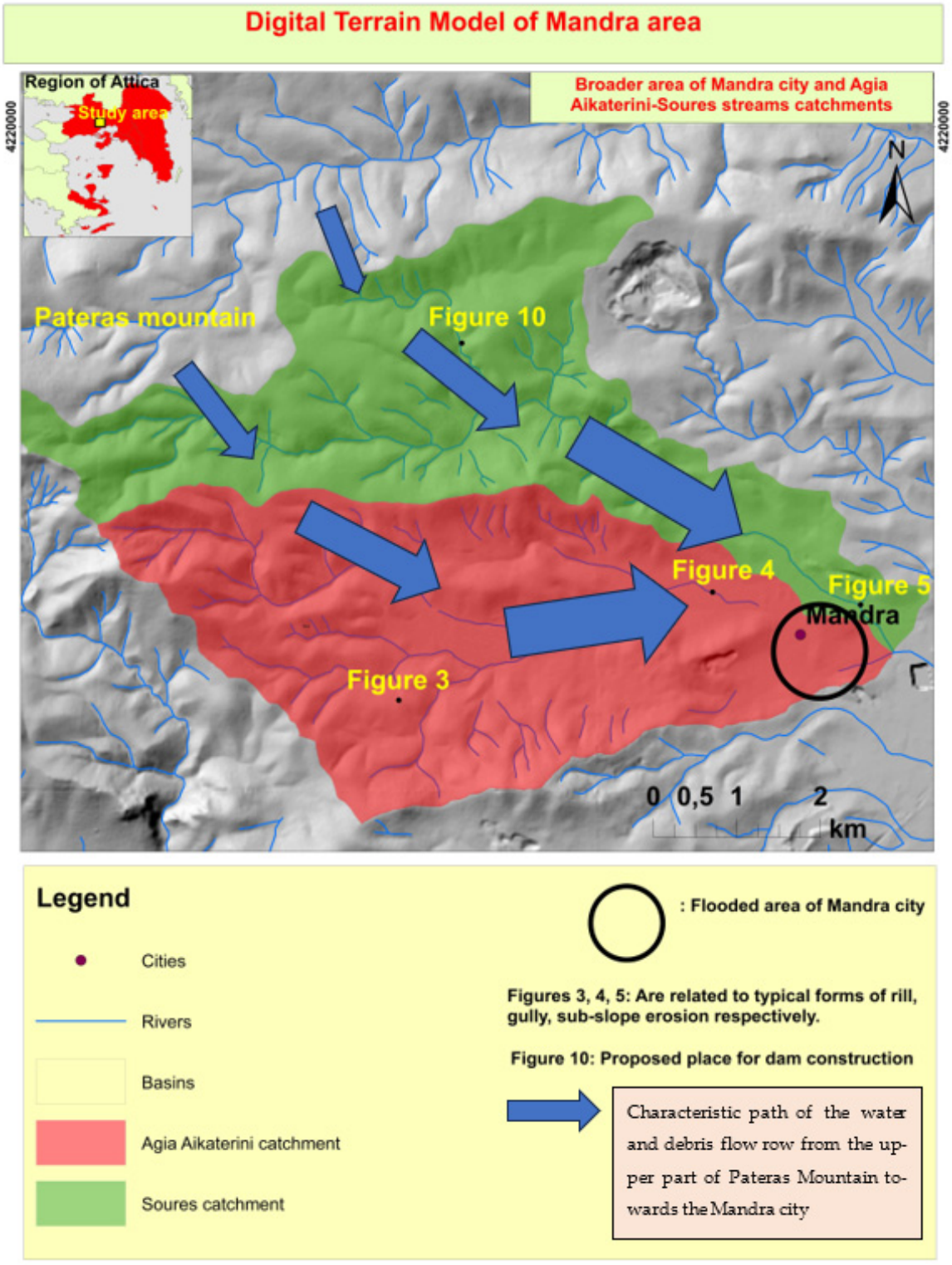

Figure 1. The case study of the Mandra fatal flash flood (2017). The boundaries of the catchment areas in the wider study area are presented [53]. In addition, the location of Figures 3, 4, 5, and 10 is correlated with the photos each figure depicts.

2.2. The fatal flash flood event of Mandra (11/2017).

On Tuesday 14/11/2017 heavy rainfall occurred in the wider area of western Attica (in Greece), which continued with intensity on Wednesday 15/11/2017. The total amount of rainfall in the core of the event (Pateras Mountain) exceeded 200 mm over a period of 6 hours with the highest intensity

Preprints (www.preprints.org) | NOT PEER-REVIEWED | Posted: 11 October 2023 doi:10.20944/preprints202308.0978.v2

mainly at 5:00 to 8:00 on 15/11, representing a very heavy and relatively short rainfall. A remarkable fact of the flooding episode was the great rapidity that was recorded. As a result, increased water flow and the consequent cause of erosion and solid discharge entered the settlement of Mandra, causing extensive damage to houses, and roads and the death of twenty-four (24) people. The study area (a part of it, is depicted in Figure 2) covers the catchment areas of the two streams Agia Aikaterini and Soures located upstream of the settlement of Mandra [54].

Figure 2. Two views from the fatal flash flood. On the left a picture of the flood zone in the Mandra city is depicted (in rectangular shape), delivered by the Copernicus Emergency Management Service-Mapping [54] and on the right a characteristic view of the flooded Mandra-Elefsina road [55].

2.3. Geological setting

The main lithostratigraphic characteristics of the formations found in the study area from the latest to the oldest are as follows: (α) Alluvial deposits, (b) Modern lateral deposits, (c) Old alluvial deposits, (d) Marls, clays, sandstones, travertines, marly limestones and conglomerates, (e) Limestones, (f) Dolomitic limestones [53]. In addition, the study area contains some faults and a well-developed hydrographic network. The geological mapping in the catchments of the two streams that run through and north of the settlement of Mandra, provided useful information about the geological formations, their specific physical characteristics and their tectonic stress. This information is decisive for determining the extent of the contribution of each formation to the creation of flood conditions and increased supply of sediment of various sizes in the area. More specifically, the largest part of the catchments, which is the mountainous part, is made up of dolomites and dolomitic limestones, which are highly fragmented, resulting in crumbling and creating mantles of alteration. The fractures and foliations of the fragmented rocks decrease their mechanical strength and increase the capability of generating loose geomaterials which lead to the formation of soil through the process of erosion. In addition, the erosivity of rainfall and run-off were the main causes for loosening the weathering mantle of decomposed – fragmented rocks, resulting in weakening of the slopes and as a result leading to mass movements of solid and semi-solid materials. All these materials can be easily eroded and in the event of heavy rainfall can provide materials for transport by water through streams.

2.4. On site geological findings

The smoothest part of the catchment areas (lowland) consists of deposits, i.e., materials that have been deposited in these areas in an earlier geological time (Upper Pleistocene), and their deposition process is similar to the process that deposited the sedimentary materials during the flood event of 15 November 2017 [53]. That is, it was found that there were several successive flood events in the area in the recent geologic past that created the deposits in the lowland sections. These materials by water movement and by mechanical means have been welded together, forming very cohesive horizons, which are impervious to water, but also very resistant to erosion. These cohesive horizons

 doi:10.20944/preprints202308.0978.v2

are found in the lowlands at depths ranging from a few centimeters (20-50), i.e., below the soil mantle, to a maximum of 1 to 3-4 m. The presence of these cohesive horizons prevents streams from digging their beds deeper, so that in the event of increased flow, their cross-section is insufficient to drain the water. Consequently, they become overflowing, and the water flows uncontrollably over the surface of the adjacent areas, resulting in the creation of many furrows or small depressions that erode the soil mantle, adding new material to the solids [53]. Based on the above observations, it is considered appropriate to provide interventions at critical points in the hydrographic network that will limit the potential for erosion from streams and downstream transport of erosion materials. In addition, in the lowland parts of the basins, where streams are unable to create a bed of sufficient cross-section due to the cohesive underlying materials, or where the bed is almost non-existent, it is necessary to define the stream and to regulate it by creating a bed of sufficient cross-section. This can be done either by excavation or by creating artificial raised walls on the sides of the streams. The geological engineering characteristics of the formations that form the basin of the Mandra area as well as their susceptibility to erosion were studied, in order to estimate the solid transport. The assessment of solid transport is very important for the planning and management of protection measures. The approximation of the total solid transport of the considered catchments, is based on the calculation of the loss of soil mass by means of the measured erosion forms and on the other hand in the calculation of the total volume of the flood deposits, the extent of which was mapped by means of high-resolution satellite imagery and in situ measurements [53].

Preprints (www.preprints.org) | NOT PEER-REVIEWED | Posted: 11 October 2023 doi:10.20944/preprints202308.0978.v2

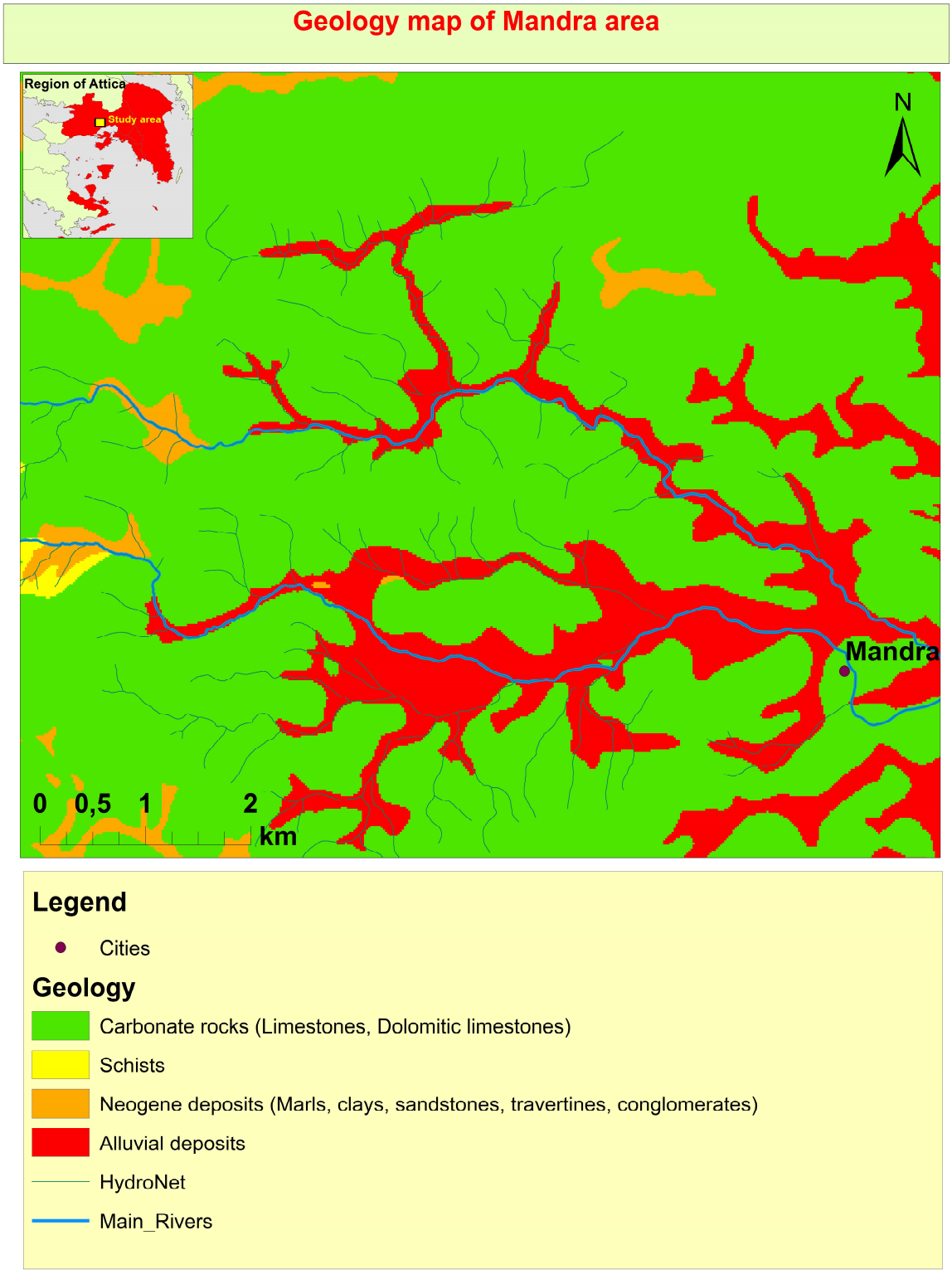

Figure 2. c. Geological map of Mandra area.

2.5. Causes of the Mandra flood.

The main causes of the catastrophic flood were [53]:

1) urbanization, which significantly increases flood risk as it leads to the impairment of critical stream cross-sections

2) the complete disappearance of small watercourses or their conversion into roads or parking places

 doi:10.20944/preprints202308.0978.v2

3) the construction of sub-dimensioning projects, that cannot take the hydraulic load in cases of heavy rainfall, as in the case of Mandra

4) the dramatic reduction in the capacity of the soil to absorb part of the rainwater; and finally

5) the very high concentration of atmospheric precipitation in a small area (such as that of Mandra) and the intensity of the rainfall

This localized rainfall which occurred in the mountainous parts of the region caused a flash flood in the catchments of the area and specifically the streams that flow into the lowland area of Mandra and the industrialized area of Mandra. These streams activated alluvial riffles formed by the supply of sediments within the Quaternary, resulting in flooding with a large amount of sediment. The areas inundated by water are located on top of the geological formations of the ripples. The development of settlements perpendicular to the water flow and on these alluvial ridges cut off the smooth drainage of water to the sea, resulting in water flooding the settlements. The development of roads and railways perpendicular to the flow is also estimated to have cut off the smooth drainage, resulting in the floodwaters being amplified in width.

2.6. Soil erosion - Erodibility

Soil erosion or soil loss is the amount of soil or rock material that becomes detached under the influence of rainfall and subsequent surface runoff over a given period [9]. In our case, the soil erosion process happened due to extremely heavy rainfall, runoff, and gravity [53]. Research claims the fact that soil erosion is extremely sensitive to rainfall [56,57]. The process of water erosion leads to decomposing, transportation and deposition of sediment in a separate place. Erosion depends on factors such as [53]: (i) the erosivity of the water (rainfall intensity, volume and kinetic energy of the flow), (ii) morphological gradients, (iii) the presence or absence of vegetation cover, (iv) the resistance of the soil to erosion (erodibility), (v) climatic conditions and (vi) human interference: natural soil erosion is locally accelerated with anthropogenic interventions (road construction in stream beds, embankments, etc.), which disturb the soil structure and produce loose materials. The total land loss during the flood event of November 2017, amounted to more than 150.000 m^3 [53]. The heavy rainfall that led to the catastrophic flood of 15 November 2017 in the urban area of Mandra was also accompanied by extensive soil erosion in large parts of the examined catchments. Soil erosion by water includes two main phases: the detachment of soil particles and their subsequent transport by water flow. When the transport energy of the water is reduced (reduction in flow rate, reduction in flow surface slope, etc.), the deposition phase of the transported materials follows. The typical forms of soil erosion that have occurred in the Mandra catchments and have led to extensive solid transport are as follows [53]: (a) Surface (sheet) erosion, (b) Rill erosion, (c) Gully erosion, (d) Slope and sub-slope erosion.

2.6.1. Surface (sheet) erosion

Surface erosion is caused by the detachment of aggregates or soil components by raindrops [53]. Some of the detached particles move through the hydrological network, while others are deposited lower down. The erosive capacity of raindrops depends on their kinetic energy and momentum, which is a function of the size of the droplets combined with the direction, intensity of the rainfall, and their final velocity. The resistance of soils to erosion (erodibility) also plays an important role in the action of the raindrop. Not weathered rocks and cohesive soils have a low susceptibility not only to surface erosion but also to all forms of erosion. Soils covered by vegetation are largely protected from erosion. Soil loss also increases significantly with increasing slopes of the morphological relief. Surface erosion, although less visible, is an important factor in soil loss due to the destruction of the soil structure, which is then easily washed away by surface runoff.

Although the calculation of the total soil loss due to surface erosion in the Mandra catchments requires systematic measurements over a super-annual period, it is estimated that its contribution to the production of solids during the phase of the intense rainfall episode (14-15/11/2017) was much lower compared to the following forms of erosion. The reason is that the topographically higher parts of the catchments, where the rainfall intensity is highest, are structured by carbonate rocks, which

Preprints (www.preprints.org) | NOT PEER-REVIEWED | Posted: 11 October 2023 doi:10.20944/preprints202308.0978.v2

generally exhibit low erodibility.
In addition, most of the basins are covered by vegetation, which acts as a protection against surface erosion.

2.6.2. Rill erosion

Rill erosion is a development of surface (sheet) erosion and is caused by the concentration of rainwater, which cannot percolate down to the subsoil, in small soil cavities, which progressively overflow and form irregular longitudinal surface runoff [53]. As the volume of runoff gradually increases, both the carrying capacity of the already extracted material and the potential for new material to be extracted along the water path increases. The erosive power of water depends on the volume, velocity, and rate of supply of surface runoff, slope gradient and soil erodibility. This creates many, small and shallow (<1m) rills that follow the direction of maximum slope of the soil surface, forming water flow axes of usually triangular cross-section. The resulting sedimentary material is coarser than that produced by surface erosion and consists mainly of medium-sized gravels and coarse sand. The development of rill erosion in the catchment area of Mandra, is particularly pronounced in areas structured by the engineering geological unit of Holocene deposits, where vegetation is also absent (Figure 3).

Figure 3. This photo shows rill erosion on Holocene deposits of the Mandra hydrological basin, and it is located in Figure 1.

2.6.3. Gully erosion

This type of erosion is developed by the flow of water along the axes of the maximum slope gradient of the slopes, where gullies of more than one meter in depth are formed [53]. The mechanism of their formation is like that of rill erosion, but on a larger scale, due to the greater concentration of water and the increase in its erosive and transport energy. The cross-section of the trenches depends on the erodibility of the soil with depth. In easily corroded materials, there is usually continuous dredging, and the cross-section is typically triangular, but deep erosion slows down considerably when the bottom of the trench reaches a corrosion-resistant formation. In this case, erosion progresses mainly laterally, and the cross-section of the gully is U-shaped. In the catchments of the Mandra rivers (e.g., Agia Aikaterini and Soures), intense trench erosion developed after the heavy rainfall that occurred on 14-15/11/2017, which contributed significantly to the production of fine and medium size sediment. Gully erosion developed in the upper and mainly in the middle elevations of the two basins, especially along valleys with a strong gradient, where the increased water volume significantly increased its erosive energy. Typical forms of gully erosion in the Mandra catchments are shown, which were developed mainly within the Holocene deposits (Figure 4).

Preprints (www.preprints.org) | NOT PEER-REVIEWED | Posted: 11 October 2023 doi:10.20944/preprints202308.0978.v2

Figure 4. Those photos (e.g., 4a, 4b) show typical forms of gully erosion developed on Holocene deposits of the Mandra hydrological basin and it is located in Figure 1.

2.6.4. Slope and sub-slope erosion (Riverbank erosion)

In the central beds of the streams of the two catchments of the Mandra and as the elevations and gradients decrease, gully erosion develops into slope and sub-slope erosion taking the form of a riverbank erosion feature (Figure 5). The strong flow of stream water detaches and carries materials from the foot of the slopes downstream, widening or deepening the bed [53]. The amount of erosion depends on the force of the water, the slopes of the bed, the meanders and bends it creates, and the erodibility of the geological formations through which the stream flows. The presence of vegetation or the local accumulation of coarse material in the streambed often diverts the main flow of the stream towards the slope, resulting in severe erosion. Slope and sub-slope erosion can be localized, as they usually develop perpendicular to the flow direction of the stream. Sub-slope erosion also is also created in the bed of streams, in places of abrupt changes in elevation, where small waterfalls are formed. These forms of erosion can be observed in almost all the main and some secondary branches of the hydrological network of the Mandra catchment areas. The intense runoff that caused the major flooding in Mandra in November 2017 led to extensive slope and sub slope erosion, resulting in the large widening of stream valleys and the removal of large volumes of material that were transported downstream. The slope and sub-slope erosion in the Mandra basin, primarily affects the Holocene deposits of the stream slopes, but at a second level also the Pleistocene deposits, with differential erosion of the less cohesive horizons.

Preprints (www.preprints.org) | NOT PEER-REVIEWED | Posted: 11 October 2023 doi:10.20944/preprints202308.0978.v2

Figure 5. Those photos (e.g., 5a, 5b, 5c, 5d, 5e), show typical forms of slope and sub-slope erosion developed on Holocene deposits of the Mandra hydrological basin and they are located in Figure 1.

2.7. Modeling of Soil Erosion.

2.7.1. Susceptibility to soil erosion

The movement of soil is a sign of a soil erosion hazard. This includes riverbank erosion, gully erosion, debris-falls, rock-falls, and generally slope failures that can create damage to the environment and human beings [3]. Annually, more than thousands of lives are lost due to mass soil movement worldwide [58]. However, Blaschke et al. [59] mention that the impacts of mass movements on soil erosion and land productivity are underestimated in the literature. Thus, less research attention was given on soil erosion due to the mass movement. Most of the soil erosion

 doi:10.20944/preprints202308.0978.v2

hazards prevail during a rainy season or after heavy rain [60,61]. Therefore, realizing the susceptibility to soil erosion is very important for mitigation and hazard - risk minimization. In order to investigate the intensity and erosion that can be seen in the examined area of Mandra, a particular methodology was implemented by Regional Authority of Attica/Directorate of Technical Works, and Hellenic Survey of Geological and Mining Exploration (H.S.G.M.E). [53], as follows.

To begin with, the erosivity of surface runoff (such as the one derived from the flash flood on 14-15 of November 2017), as well as the erodibility of the geological formations in the broader area of Mandra, determine how susceptible the geoenvironment is to the creation of gully [14,15], a type of soil erosion that is appeared in the examined area of Mandra.

Soil erosion map derived by a research project that accomplished by Hellenic Survey for Geology and Mineral Exploration (H.S.G.M.E.) in 2018, under the auspices of Technical Authority of Attica Region, which supervised this project [e.g., checking, reviewing, and approving the deliverables (e.g., technical reports and cartographic products)]. The process of how those soil erosion lines were delineated, is described more analytically in the following lines. The soil erosion map was produced based on the synthesis of three individual maps: (a) the engineering geological map, (b) the vegetation map, (c) the morphological (slope) map.

Concerning the first map, the engineering geological map examined and classified the formations that structure the area, according to their lithological composition and hydrogeological behavior. The influence of tectonics was considered using the existing hydrographic network. Geological data were taken from the literature and supplemented by field surveys. For the soil erodibility map, the role of lithological composition, infiltration capacity and permeability were considered.

Infiltration is a property of soils. Continuous infiltration can result in saturation of the soil cover or weathering mantle. In the area under consideration, this property is very important, because Neogene formations and weathering mantle can be saturated by prolonged rainfall and then become loose and easily eroded.

There should be no confusion between the concepts of permeability (which is a measure of the ability of the formation to allow water to pass through its mass) and infiltration, i.e., the ability of water to percolate through the soil mass without necessarily moving to a depth to reach the water table. Infiltration refers to soils and not to rocks, where usually if infiltration is present, it is referred to as deep percolation. In soils, continuous infiltration leads to saturation. The role of the soil cover on the rocks, which is usually a decomposed, clayey mantle with permeability, is therefore very important. The existence and thickness of the ground cover were estimated from field observations, particularly in areas recently affected by extensive forest fires, and from the 1:50 000 scale soil maps of the Institute of Forestry Research [53,62].

Regarding the second (vegetation) map, the land use is based on mechanical and hydrological characteristics as well as vegetation in order to control the slope stability [63–65]. During rainfall, land use influences the behavior of the soil as well as the magnitude of potential geomaterial that is about to move. In this case study, the land use classification was used from the research of Tavoularis et al. [51], where five classes identified: (i) Barren areas, (ii) Urban areas, (iii) Forest areas, (iv) Shrubby areas-Natural grassland and (v) Cultivated areas. For the necessity of this work, the barren area class was implemented in order to estimate the soil erosion susceptibility.

Finally, considering the third (morphological/slope) map, the value of the slope was chosen to be 5%, because this value is mentioned in the literature as the limit of the processes of deposition of fractional materials, in conditions of diffuse flow (mudflow) and sedimentation on the surface of the earth (creation of cones of craters). The slope map distinguishes between areas with a slope of more than 5 %, where erosion processes are more intensive, and areas with a slope of less than 5 %, where erosion processes are less severe [53,62].

Thus, the susceptibility to erosion of the geological formations of Mandra was assessed based on the observations of the technical geological mapping, the erosion phenomena observed and recorded in the wider catchment area (from technical – site investigations in 2017, 2018, 2022), combined with the physical and mechanical characteristics of the geological formations. The grading

 doi:10.20944/preprints202308.0978.v2

of the units was carried out based on their physical and mechanical characteristics and estimated permeability.

In the present case study, the most interesting unit (associated with the highest soil erodibility) was the Holocene deposits, which cover an area of 2.05 km^2 [53]. Those geomaterials derived from river deposits, are brown to reddish-brown in color, generally loose to slightly cohesive, covering the smooth parts of the catchment. They originate from the erosion of older formations and deposition by surface runoff and gravity. They comprise mixed phases of materials, with a corresponding average proportion of coarse to fine-grained materials and rapid changes in grain size during both horizontal and vertical development. In places they may represent lateral or alluvial deposits. Their thickness varies locally from a few centimeters to two meters, but is usually in the order of 50 cm. The coarse phase consists mainly of mudstones, gravels, and coarse-grained sands of mainly dolomitic and calcareous composition. The fine phase, which is the binder, consists mainly of sandy to silty sands (CL, SC) with a variable but generally small proportion of clay. They are characterized as soft to medium cohesive soils and rarely very soft or stiff. The plasticity of the soils is generally low. They are characterized by low to medium water permeability and very high erodibility.

The above (three) parameters are the criteria for assessing the susceptibility to soil erosion and assuming equivalent weighting and linear correlation between them, the thematic maps were superimposed and the corresponding susceptibility map in the Agia Aikaterini and Soures catchments was obtained. Moreover, the previously mentioned findings are in line with Hydroment Associate's site-investigation work (2021) in those two examined watersheds (Agia Aikaterini and Soures), which was executed under the auspices of Region of Attica's Authority, which is responsible for designing and implementing mitigation measures against flooding [66]. The combination of the three final maps produced the erosivity map, part of which is depicted as soil erosion lines in the following map (Figure 6).

The described soil erosion lines validated not only on-site by technical visits executed by Technical Authority of Attica Region (2017, 2022), but also using an already web-GIS landslide susceptibility map, the creation of which accomplished via a research project briefly entitled "DIAS" [51]. Specifically, the generated soil erosion lines overlaid to the landslide susceptibility map, showing that those lines achieve a consistent coincidence with the zones of "Extremely high (slope failure) susceptibility" and "Landslide".

The above-mentioned soil erosion types recorded during the in-field site investigation were validated through an already generated landslide susceptibility map [51], which is shortly described in the next section. In this map, a strong correlation between the defined soil erosion lines and the landslide susceptibility zones that come up from a semi-quantitative methodology named Rock Engineering System (RES) was confirmed.

Preprints (www.preprints.org) | NOT PEER-REVIEWED | Posted: 11 October 2023 doi:10.20944/preprints202308.0978.v2

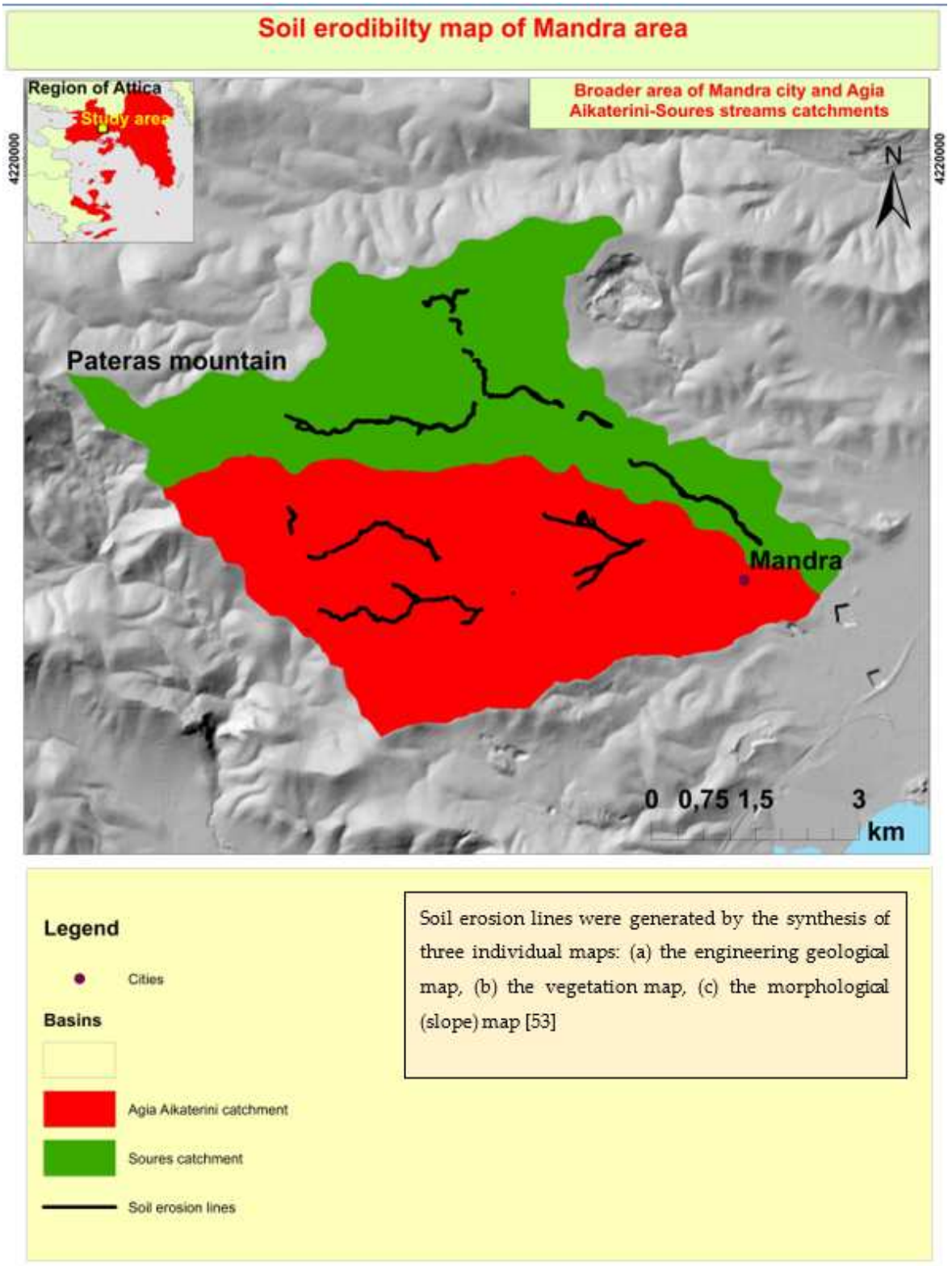

Figure 6. Soil erodibility map of Mandra study area [53].

2.7.2. Rock Engineering System (RES) methodology.

This approach is mainly based on the correlation of mechanisms between landslide parameters through a matrix-table and uses slope failure factors that can potentially be identified during the preparation phase of a preliminary, final or implementation study of a civil engineering project. The scope of using RES, is to estimate the landslide instability index which results in generating landslide

Preprints (www.preprints.org) | NOT PEER-REVIEWED | Posted: 11 October 2023 doi:10.20944/preprints202308.0978.v2

susceptibility, hazard, and risk maps [51]. RES is a semi-quantitative rock engineering approach and the basic tool for representing the parameters and their interaction mechanisms (Figure 7). It is based on an interaction matrix that represents the key parameters, as leading diagonal terms, and their binary interaction mechanisms as off-diagonal terms. RES was developed by Hudson in 1992 [67] to determine the interaction of several parameters in rock engineering design and calculate the instability index for rock slopes. Since then, it has been modified and applied to rock stability problems, landslide susceptibility analysis and rock engineering [68]. Thus, by implementing RES methodology expert defines the most important causative and triggering factors responsible for the slope failures, quantifies their interactions, obtain their weighted coefficients, and calculates the instability index, which refers to the potential instability of the examined natural slope.

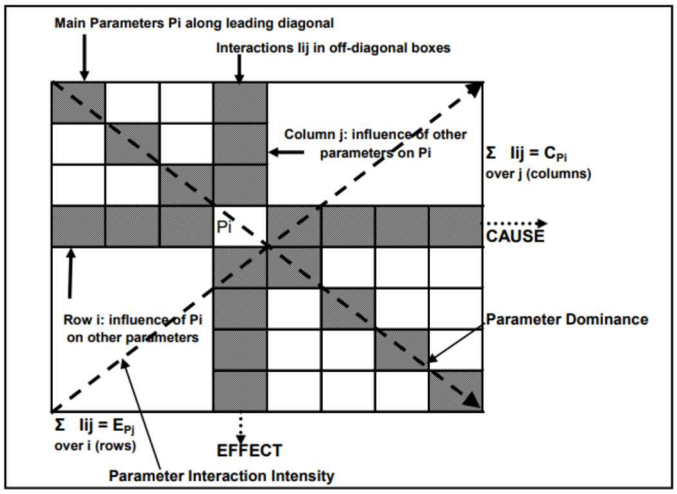

Figure 7. RES interaction matrix-table [68–70].

The estimation of landslide susceptibility index is based on a series of subsequent actions, such as: a) Selection και rating of (landslide) parameters, b) Construction of interaction matrix, c) Coding of binary interaction among the selected (landslide) parameters, d) Construction of Cause – Effect diagram (The cause-effect plot is helpful to understand the role of each landside factor to slope stability analysis), e) Calculation of weighting coefficient of each parameter and f) Estimation of (landslide) instability index. In Tavoularis et al. [51] research (or briefly DIAS project), ten parameters were used as independent controlling factors to model the landslide susceptibility. These factors, which were utilized for the RES methodology, were: (i) Distance from roads, (ii) Land use, (iii) Slope inclination, (iv) Slope orientation (aspect), (v) Lithology, (vi) Hydrogeological conditions, (vii) Rainfall, (viii) Elevation, (ix) Distance from streams and (x) Distance from tectonic elements.

3. Results

This (landslide susceptibility) map was generated in a GIS environment (specifically ArcGIS 10.2.2, which is a product of ESRI company), using the already mentioned thematic layers (e.g.,: distance from roads, land use, slope inclination, aspect, lithology, hydrogeological conditions, rainfall, elevation, distance from streams, distance from tectonic elements). The data used for the preparation of these layers were obtained from different geodata sources among which are a mosaic geological map from the Hellenic Survey of Geological and Mineral Exploration and the Digital Elevation Model from Hellenic Cadastre S.A. [51].

Afterwards, every data layer was digitized and converted into grids with a cell size of 20 x 20 m. Furthermore, weights and rank values to the reclassified raster layers and to the classes of each layer were assigned, respectively, taking into consideration the previously mentioned methodology of RES. Finally, the weighted raster thematic maps were multiplied by the corresponding weights and added up (via a tool of ArcGIS tool, namely "weighted sum") to generate the slope failure map where

Preprints (www.preprints.org) | NOT PEER-REVIEWED | Posted: 11 October 2023 doi:10.20944/preprints202308.0978.v2

each cell has a particular index value regarding landslide susceptibility. The reclassification of this map represented the final susceptibility map of the examined area of Attica Region, divided into susceptibility zones according to Brabb et al. classification [71]. The landslide susceptibility index (LSI) values in the final susceptibility map were classified into (e.g., five) categories, namely "Low-Middle", with Instability index (Ii) < 25, "High" with 25 < Ii < 42, "Very High" with 42 < Ii < 53, "Extremely high" with 53 < Ii < 70", and "Landslide" with Ii > 70%. From this classification, the main point that derives is, that the higher the LSI, the more susceptible the area is to landslides (instability index higher than 70%).

Ultimately, the generated landslide susceptibility map for the entire county of Attica Region is the following (Figure 8). The map has been validated using Confusion Matrix and a number of 220 slope failures [51].

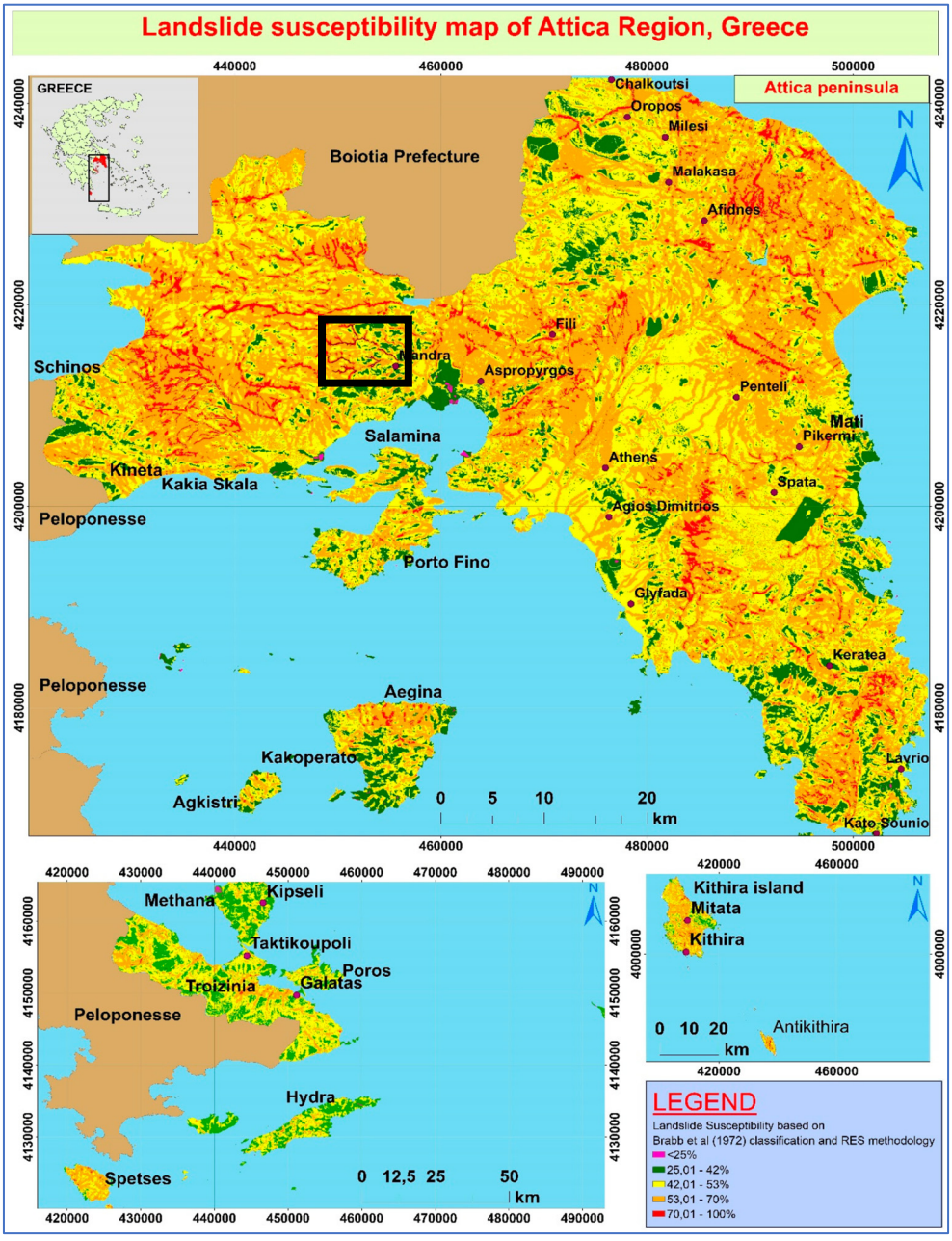

Figure 8. Landslide susceptibility map of Attica Region [51]. The landslide susceptibility index (LSI) values in the susceptibility map were classified into five categories: "Low-Middle", with Instability index (Ii) < 25 (Light green color zone in the map), "High" with 25 < Ii < 42 (Green color zone), "Very High" with 42 < Ii < 53 (Yellow color zone), "Extremely high" with 53 < Ii < 70" (Orange color zone),

Preprints (www.preprints.org) | NOT PEER-REVIEWED | Posted: 11 October 2023 doi:10.20944/preprints202308.0978.v2

and "Landslide" with Ii > 70% (Red color zone). From this classification, it can be clearly notified that the higher the LSI, the more susceptible the area is to landslides (instability index higher than 70%). The area inside the black rectangular scheme, corresponds to the present study (Mandra area).

The generated landslide susceptibility map can be used with the already produced potential highly flood hazard zoning maps of Attica Region authorized by the Greek Ministry of Environment and Energy, and with the produced flooded area maps, delivered by the Copernicus Emergency Management Service-Mapping [54]. The outcome of the DIAS project is accessible to the public, through an open-access web-based platform (https://gis.attica.gov.gr/en/node/1216), so as to aid awareness of landslides among different stakeholders (e.g., landslide experts, government authorities, planners, decision-makers, citizens). Moreover, the DIAS project can facilitate the role of Civil Protection Authorities, by providing inputs for prevention and preparedness. For further study of the previously briefly described methodology, readers are kindly suggested to read the following relevant research [51,68–70].

3.1. Mapping performance evaluation

The aforementioned soil erosion types were subject to expert-based cross-checks and validated through on-screen visual interpretation of the generated landslide susceptibility map of the Attica Region. The soil erosion types depicted as lines and were overlaid on the landslide susceptibility map (on landslide susceptibility zones) in order to identify the correlation of potential slope failure zones with soil erosion lines (Figure 9). It was found that there is a consistent coincidence between all of the derived soil erosion lines and the areas that are characterized, regarding the landslide susceptibility, as "very high susceptibility", "extremely high susceptibility" and," Landslide", based on the generated landslide susceptibility map of Attica Region (Figure 8) and Brabb et al. [71].

The verification was executed by implementing a frequency ratio statistical analysis, where the relationship between spatial distribution of landslide susceptibility zones and soil erosion lines was studied. Specifically, the ratio is that of the area where soil erosion lines manifested to a particular landslide susceptibility zone. According to Pradhan et al. [35], a value of 1 is an average value. A value lower than 1, means lower correlation of occurring soil erosion lines, whereas a value greater than 1, it means a higher correlation.

All the derived soil erosion lines were found to be into the "very high susceptibility", "extremely high susceptibility" and," Landslide" zones. To estimate the frequency ratio, the frequency distribution of soil erosion lines was calculated for each landslide susceptibility zone of the Mandra area. Moreover, the area ratio for each landslide susceptibility zone (measured in pixels), as well as the meters ratio for each soil erosion lines was computed. Finally, the frequency ratio for soil erosion lines associated with the "very high susceptibility", "extremely high susceptibility" and," Landslide" zones was calculated by dividing the frequency of soil erosion lines to the landslide susceptibility zone area (measured in pixels).

Frequency ratio generated for Mandra area is shown in Table 2. For lower probability of landslide occurrences [e.g., 42<Ii (Instability Index) <53], the frequency ratio is equal to 0,05, which indicates poor relationship between soil erosion lines and the generated landslide susceptibility zones. For extremely high landslide susceptibility (e.g., 53<Ii<70) and beyond (e.g., 70<Ii<100), the frequency ratio is found to be greater than 1, which indicates strong relationship between landslide susceptibility zones and soil erosion lines.

Table 2. Frequency ratio values of soil erosion lines into landslide susceptibility zones.

Landslide Susceptibility Zones	Pixel in domain	Pixels (%) (a)	Soil Erosion Lines (m)	Pixels (%) (b)	Frequency ratio (b/a)
42-53%	777.203	42,32	917,35	2,3	0,05
53,01-70%	933.057	50,81	21.920,1	55,11	1,08
70.01-100%	126.032	6,87	16.935,46	42,59	6,2

Preprints (www.preprints.org) | NOT PEER-REVIEWED | Posted: 11 October 2023 doi:10.20944/preprints202308.0978.v2

Total	1.836.292	100,00	39.772,91	100,00	1

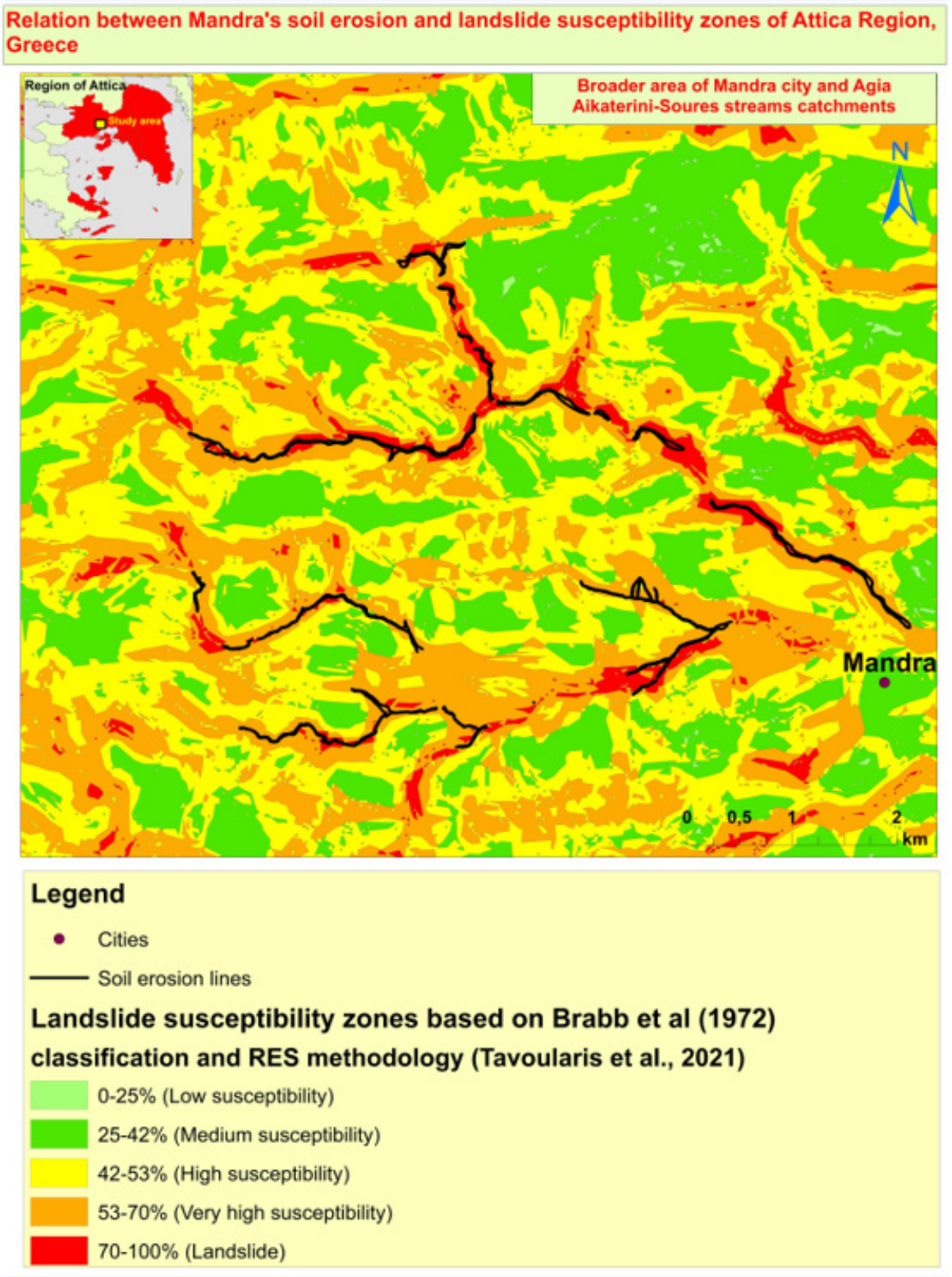

Figure 9. Focus on the area depicted in the rectangular shape of the previous (landslide susceptibility) map. Relation between soil erosion lines in black color and the "high", "very high" and "landslide" susceptibility zones.

Taking into consideration the above mentioned, that kind of landslide susceptibility model (e.g., DIAS project) could be used as a soil erosion prediction model. Since, soil erodibility reflects the soil susceptibility to erosion, accurate mapping of susceptibility to erosion hazard is crucial to avoid

 doi:10.20944/preprints202308.0978.v2

economic losses and life losses [3]. Thus, implementing the outcomes of landslide susceptibility mapping in validating soil erosion areas, can lead to identifying and consequently estimating soil erosion hazard and vulnerability.

4. Discussion

Slope failures and specifically shallow landslides contribute to land degradation (e.g., soil loss) in Europe. Thus, soil erosion and shallow landslides are the most important types of soil loss that can be observed all over the world.

Kue et al. (2020) refer that the quantitative characterization of the interaction between soil erosion and landslide is rare. So, they calculated the area and volume of 5,420 shallow loess landslides and compared these against the Chinese Soil Loss Equation (CSLE) derived soil erosion rate of 15 sub-catchments. Their analysis revealed a satisfactory linear fitting result between the area of landslides and soil erosion. In the present study, an attempt is made for the quantitative characterization of the interaction between soil erosion and landslide, using RES methodology.

In Lee et al. [34], and Pradhan et al. [35] articles, the soil erosion map was verified using the landslide locations by the integration of USLE with GIS to model the potential for soil erosion. In Rozos et al. [28] paper, the Revised Universal Soil Loss Equation (RUSLE) was implemented to predict sites susceptible to slope failures caused by soil erosion. In those three papers, the verification that was followed was the same as in the present study, which means that the generated soil erosion map was verified by comparing the soil erosion hazard zones with the spatial distribution of slope failures. Furthermore, one additional common characteristic is that the assessment of the dynamic soil erosion process can be correlated with another equally important and related threat of landslides [44]. Finally, from the above-mentioned studies, considering the present study, it can clearly be said, that by adjusting the factors which are responsible for soil erosion like lithology, land use, etc., the rate of soil erosion can be minimized. As a result, gully and landslide inventory maps are very useful in identifying the distribution of sediment sources and their landscape characteristics which are connected to their existence [44]. By defining that distribution, this study could contribute to monetary estimates, regarding the cost of removing sediments, while trying to implement flood mitigation measures towards new potential heavy rainfall episode.

In Tavoularis et al. research [51], different types of slope failures [72] manifested in the entire Region of Attica, such as falls, rockfalls, slides, debris. Among them and regarding Mandra area, shallow landslides are the most prominent type that affects that region. Shallow landslides are very much related to gradual soil erosion, since they easily affect soil materials transposed by erosion [73]. Thus, the interaction of soil erosion and slope failure processes contributes to the loss of fertile loss, and the alteration of the landscape, not to mention damages to infrastructure and human facilities. Moreover, soil erosion and shallow slope failures are important geological issues, so specific studies are crucial to generate models in order to cope with the hazard and vulnerability against these phenomena [74]. Taking into consideration the above-mentioned, a well-structured landslide susceptibility map such as that of the previously one described, may be helpful to identify and characterize areas (in this study on a regional scale) of potentially increased land degradation. That's why it is important to gather and study spatial information on soil loss interacting with slope failures.

4.1. Prevention and control actions

It is scientifically documented, legally established and empirically proven that in order to be effective in dealing with the flooding action of a stream, the study of flood control works should concern the entire catchment area and include the necessary forestry works of stream regulation, which have the following positive results [53,66]:

- a reduction in the amount of solid material transported, with a corresponding reduction in the erosive capacity of the flood waters and the volume of the flood wave.
- The velocity of the flood wave is reduced, resulting in a delay in its occurrence downstream and a reduction in its destructive momentum.
- The effects of erosion on unprotected soils are reduced.

Preprints (www.preprints.org) | NOT PEER-REVIEWED | Posted: 11 October 2023 doi:10.20944/preprints202308.0978.v2

- The natural environment is protected and enhanced, especially through planting and soil protection projects.

The types of projects proposed include the following:

- Construction of small dams to grade the bed and retain the slopes
- Construction of dams for the retention of debris
- Construction of culverts in places where the existing road network is eroded by streams in the study area
- Settlement of part of the hydrographic network of the study area by constructing an artificial bed with a dike
- Implementation of horticultural works
- Forestry measures for the management of the overall forest complex in the study area
- Opening of forest roads to reach the sites of the proposed projects

Particularly, given that the purpose of the interventions is to reduce flood risk and prevent catastrophic events, it was considered appropriate to limit the proposed measures to small dams, which are mainly of a preventive nature and aim to manage runoff effectively. These measures were considered to be the most appropriate proposal for the area, at least because they meet the requirements of being as low as possible in terms of cost and short implementation time. To be more specific, the types of the recommended dams are as follows (Figure 10):

(a) Construction of sediment barriers is intended to be between 3m and 8m high with reinforced concrete or unreinforced concrete construction material. The purpose of these dams is to counteract the axial erosion of the bottom of the stream bed, by reducing the drag force of the water and retaining the sediment.

(b) Construction of graduation dams - slope stabilization: These dams are proposed to be made of concrete (reinforced or unreinforced) or of reinforced wire mesh (e.g., sarsenet). The construction of the dams will be carried out either in places where there is evidence of gradual erosion, or in places where there is axial erosion of the bottom of the bed, in combination with the above-mentioned sediment barriers. The height of these dams according to the theoretical assessment carried out, is proposed to be between 1m and 2m.

Figure 10. From a characteristic broader view of Mandra area, a partly soil erosion degraded area (located west of capital city of Athens, Greece) where a small dam is going to be constructed for coping against future (flash) flood events [75].

5. Conclusions

This study investigated the correlation between soil erosion and land degradation (e.g., landslides) in a specific area in Attica Region (Greece). Particularly, soil erosion types were depicted

on a map over an area that suffered from flash flood that happened on November 2017 in the Mandra area. The reliability of this map was assessed by comparing the potential slope failures predictions generated in a landslide susceptibility research project (DIAS), and also validated from several field works executed for the design of flooding mitigation measures under the auspices of Directorate of Technical Works of Attica Region (Greece). The main conclusions that come up while developing this work can be summarized as follows:

1. There is a very strong correlation between soil erosion and potential landslide susceptibility zones.

2. The landslide susceptibility model (DIAS) could be used as a (preliminary) guide for investigating and identifying soil erosion issues, providing crucial information for immediate actions and long-term planning.

3. Implementing Geographical Information Systems technology provides continuous monitoring and evaluation of soil erosion susceptibility to hazard reduction.

4. This study could add value to local authorities of Mandra municipality for defining areas susceptible to soil erosion and as a result it can contribute to the design and afterwards to the construction of flooding protection mitigation measures.

5. To the author's knowledge, it has not been approached, so far, the relationship between soil erosion and landslide events using an expert semi-quantitative methodology, named Rock Engineering System (RES). Apart from the already known models that have been implemented until today (e.g., USLE, RUSLE, etc.), soil erosion identification can also be approached via a tool such as that of RES in conjunction with landslide susceptibility mapping which, in our case study, has been generated for a region of approximately 3.800 km^2, and (this map) has already been validated by 220 slope failures recorded in the last 60 years (1960-2020) in the entire region of Attica. Based on a heuristic approach, RES can combine different parameters and study the interaction of those parameters, to estimate quantitatively the instability index of an examined slope that can be associated with landslide susceptibility zones. In our case study, some of those zones, coincide with soil erosion lines. Those lines were derived not only from site investigations (in three different chronological periods: 2017, 2018, 2022) but also from a particular methodology (e.g., soil erosion susceptibility, which is described in detail in the manuscript). The conclusion is that there is an alternative way to identify soil erosion. Using RES methodology could be of great use to different stakeholders in designing the appropriate mitigation measures against phenomena such as floods and landslides. In addition, the findings of this study contribute to resilience development for future flooding protection and minimize further damages or prevent the occurrence of phenomena such as slope failures. Another useful application of this approach is the fact that this study could contribute to some monetary quantified estimates about costs of removing sediments, during the process of implementing mitigation measures against upcoming potential flood episodes.

In conclusion, the implementation of landslide susceptibility model in this study, can contribute to the online repository of scientific information in the EU Soil Observatory of the European Soil Data Centre (e.g., datasets, maps).

To this direction, the implementation of Artificial Intelligence and Machine Learning methodologies using (free) open-access Web-GIS platforms (such as those of DIAS project), accompanied with a variety of geo (including soil) data could lead to the further validation of European Landslide Susceptibility Map (ELSUS), using more accurate regional susceptibility maps through evaluation of downloaded information from European Soil Data Centre (ESDAC), succeeding in parallel to the identification, correlation and quantification between land degradation and soil erosion.

Funding: This article did not receive any specific grant from funding agencies in the public, commercial, or not-for profit sectors.

Acknowledgments: The author is grateful to the Regional Authority of Attica (Directorate of Technical Works) and Hellenic Survey for Geology and Mineral Exploration (H.S.G.M.E.), for providing valuable technical reports as well as crucial digital geodata records.

Conflicts of Interest: The author declares no conflict of interest.

References

1. Borrelli P., Poesenc, J., Vanmaerckee, M., Ballabiof C., Hervás J., Maerkera, M., Scarpa S., Panagos P. 2021. *Monitoring gully erosion in the European Union: A novel approach based on the Land Use/Cover Area frame survey (LUCAS).* International Soil and Water Conservation Research. https://doi.org/10.1016/j.iswcr.2021.09.002.
2. Panagos P., Van Liedekerke M., Jones A., Montanarella L., 2011. *European Soil Data Centre: Response to European policy support and public data requirements.* Land Use Policy 29 (2012): 329-338. Doi:10.1016/j. Landusepol.2011.07.003.
3. Senanayake S., Pradhan B., Huete A., Brennan J., 2020. *A review on assessing and mapping soil erosion hazard using geo-informatics technology for farming system management*. Remote Sensing, 2020, 12, 4063.
4. Karydas, C.G., Panagos, P., Gitas, I.Z., 2014. *A classification of water erosion models according to their geospatial characteristics*. International Journal of Digital Earth 7 (3), 229–250.
5. Teng, H., Liang, Z., Chen, S., Liu, Y., Viscarra Rossel, R.A., Chappell, A., Yu, W., Shi, Z., 2018. *Current and future assessments of soil erosion by water on the Tibetan Plateau based on RUSLE and CMIP5 climate models*. Sci. Total Environ. 635, 673–686. https://doi.org/10.1016/j.scitotenv.2018.04.146.
6. Wischmeier W., Smith D., 1978. Predicting Rainfall Erosion Losses: *A Guide to Conservation Planning. Agricultural Handbook No. 537*. U.S. Department of Agriculture, Washington DC, USA.
7. Renard K.G., et al., 1997. *Predicting Soil Erosion by Water: A Guide to Conservation Planning with the Revised Universal Soil Loss Equation (RUSLE)* (Agricultural Handbook 703). US Department of Agriculture, Washington, DC, pp.404.
8. Panagos P., Borrelli P., Poesen J., Ballabio C., Lugato E., Meusburger K., Montanarella L., Alewell C., 2015. *The new assessment of soil loss by water erosion in Europe*. Environmental Science & Policy 54 (2015) 438–447. http://dx.doi.org/10.1016/j.envsci.2015.08.012.
9. Senanayake S., Pradhan B., Huete A., Brennan J., 2020. *Assessing soil erosion hazards using land-use change and landslide frequency ratio method: a case study of Sabaragamuwa Province, Sri Lanka*. Remote Sensing, 2020, 12, 1483.
10. Batista, P.V.G., Davies, J., Silva, M.L.N., Quinton, J.N., 2019. *On the evaluation of soil erosion models: are we doing enough? Earth Sci. Rev. https://doi.org/10.1016/j.earscirev.2019.102898*
11. Gholami, V., Sahour, H., Hadian, A., Mohammad, A., 2021. *Soil erosion modeling using erosion pins and artificial neural networks. Catena 196, 104902. https://doi.org/10.1016/j.catena.2020.104902*.
12. Cohen, M.J.; Shepherd, K.D.; Walsh, M.G. *Empirical reformulation of the universal soil loss equation for erosion risk assessment in a tropical watershed*. Geoderma 2005, 124, 235–252.
13. Arabameri, A.; Pradhan, B.; Rezaei, K.; Yamani, M.; Pourghasemi, H.R.; Lombardo, L. *Spatial modelling of gully erosion using evidential belief function, logistic regression, and a new ensemble of evidential belief function-logistic regression algorithm*. Land Degrad. Dev. 2018, 29, 4035–4049.
14. Conforti, M.; Aucelli, P.P.C.; Robustelli, G.; Scarciglia, F. *Geomorphology and GIS analysis for mapping gully erosion susceptibility in the Turbolo stream catchment (Northern Calabria, Italy)*. Nat. Hazards 2011, 56, 881–898.
15. Conoscenti, C.; Angileri, S.; Cappadonia, C.; Rotigliano, E.; Agnesi, V.; Märker, M. *Gully erosion susceptibility assessment by means of GIS-based logistic regression: A case of Sicily (Italy)*. Geomorphology 2014, 204, 399–411.
16. Arabameri, A.; Cerda, A.; Tiefenbacher, J.P. *Spatial pattern analysis and prediction of gully erosion using novel hybrid model of entropy-weight of evidence.* Water 2019, 11, 1129.
17. Arabameri, A.; Cerda, A.; Pradhan, B.; Tiefenbacher, J.P.; Lombardo, L.; Bui, D.T. *A methodological comparison of head-cut based gully erosion susceptibility models: Combined use of statistical and artificial intelligence.* Geomorphology 2020, 359, 107136.
18. Meliho, M.; Khattabi, A.; Mhammdi, N. *A GIS-based approach for gully erosion susceptibility modelling using bivariate statistics methods in the Ourika watershed*, Morocco. Environ. Earth Sci. 2018, 77, 1–14.
19. Rahmati, O.; Haghizadeh, A.; Pourghasemi, H.R.; Noormohamadi, F. *Gully erosion susceptibility mapping: The role of GIS-based bivariate statistical models and their comparison*. Nat. Hazards 2016, 82, 1231–1258.
20. Angileri, S.E.; Conoscenti, C.; Hochschild,V.; Märker, M.; Rotigliano, E.; Agnesi,V.. *Water erosion susceptibility mapping by applying Stochastic Gradient Treeboost to the Imera Meridionale River Basin (Sicily, Italy)*. Geomorphology 2016, 262, 61–76.
21. Svoray, T.; Michailov, E.; Cohen, A.; Rokah, L.; Sturm, A. *Predicting gully initiation: Comparing data mining techniques, analytical hierarchy processes and the topographic threshold.* Earth Surf. Process. Landf. 2012, 37, 607–619.

22. Eustace, A.H.; Pringle, M.J.; Denham, R.J. *A risk map for gully locations in central Queensland, Australia*. Eur. J. Soil Sci. 2011, 62, 431–441.
23. Rahmati, O.; Tahmasebipour, N.; Haghizadeh, A.; Pourghasemi, H.R.; Feizizadeh, B. *Evaluation of different machine learning models for predicting and mapping the susceptibility of gully erosion*. Geomorphology 2017, 298, 118–137.
24. Arabameri, A.; Rezaei, K.; Cerda, A.; Lombardo, L.; Rodrigo-Comino, J. *GIS-based groundwater potential mapping in Shahroud plain, Iran. A comparison among statistical (bivariate and multivariate), data mining and MCDM approaches*. Sci. Total Environ. 2019, 658, 160–177.
25. Pourghasemi, H.R.; Yousefi, S.; Kornejady, A.; Cerdà, A. *Performance assessment of individual and ensemble data-mining techniques for gully erosion modeling.* Sci. Total Environ. 2017, 609, 764–775.
26. Yang A., Wang C, Pang G, Long Y, Wang L., Cruse R.M. and Yang Q. *Gully Erosion Susceptibility Mapping in Highly Complex Terrain Using Machine Learning Models*. ISPRS Int. J. Geo-Inf. 2021, 10, 680. https://doi.org/10.3390/ijgi10100680.
27. Huang, F., Chen, J., Du, Z., Yao, C., Huang, J., Jiang, Q., Chang, Z., Li, S., 2020. *Landslide susceptibility prediction considering regional soil erosion based on machine-learning models*. ISPRS Int. J. Geo-Inf. 9 https://doi.org/10.3390/ijgi9060377.
28. Rozos D., Skilodimou H., Loupasakis C., Bathrellos G., 2013. *Application of the revised universal soil loss equation model on landslide prevention. An example from N. Euboea (Evia) Island, Greece*. Environ Earth Sci (2013) 70:3255-3266. DOI 10.1007/s12665-013-2390-3.
29. Brunsden, D., & Prior, D. B., 1984. *Slope instability*. Wiley, Singapore.
30. Lim, R. P.,&Lee, S. W., 1992. *Hill development*. In Proceedings of the Seminar, Malaysian Nature Society, Kuala Lumpur.
31. Gartner, J.E., Bigio, E.R., Cannon, S.H., 2004. *Compilation of postwildfire runoff-event data from the western United States*. Open- File Report (United States Geological Survey) 04-1085, (http://pubs.usgs.gov/of/2004/1085.html).
32. Poesen, J. 2018. *Soil Erosion in the Anthropocene: Research Needs.* Earth Surf. Processes Landf., 43, 64–84.
33. Nyssen, J.; Poesen, J.; Moeyersons Layeten, E.; Veyret-Picot, M.; Deckers, J.; Haile, M.; Govers, G. 2002. *Impact of Road Building on Gully Erosion Risk: A Case Study from the Northern Ethiopian Highlands.* Earth Surf. Processes Landf. 1283, 1267–1283.
34. Lee S., 2004. *Soil erosion assessment and its verification using the universal soil loss equation and geographic information system: a case study at Boun, Korea*. Environ Geol 45:457–465.
35. Pradhan B, Chaudhari A, Adinarayana J, Buchroithner MF., 2012. *Soil erosion assessment and its correlation with landslide events using remote sensing data and GIS: a case study at Penang Island, Malaysia*. Environ Monit Assess 184:715–727. https://doi 10.1007/s10661-011-1996-8.
36. Yuan-jun J., Alam M., Li-Jun S., Umar M., Sadiq S., Jia Jia L., 2022. *Rahman M. Effect of root orientation on the strength characteristics of loess in drained and undrained triaxial tests*. Engineering Geology 296 (2022) 106459. https://doi.org/10.1016/j.enggeo.2021.106459.
37. Lian, B., Peng, J., Zhan, H., Huang, Q., Wang, X., Hu, S., 2020. *Formation mechanism analysis of irrigation-induced retrogressive loess landslides.* Catena 195, 104441.
38. Swanson, F.J., Dyrness, C., 1975. *Impact of clear-cutting and road construction on soil erosion by landslides in the western Cascade Range*, Oregon. Geology 3, 393–396.
39. Wang, X., Wang, J., Zhan, H., Li, P., Qiu, H., Hu, S., 2020. *Moisture content effect on the creep behavior of loess for the catastrophic Baqiao landslide*. Catena 187, 104371.
40. Shen, P., Zhang, L.M., Chen, H., Gao, L., 2017. *Role of vegetation restoration in mitigating hillslope erosion and debris flows.* Eng. Geol. 216, 122–133.
41. Wu, L., Zhang, L.M., Zhou, Y., Xu, Q., Yu, B., Liu, G., Bai, L., 2018. *Theoretical analysis and model test for rainfall-induced shallow landslides in the red-bed area of Sichuan*. Bull. Eng. Geol. Environ. 77, 1343–1353.
42. Acharya G., Cochrane T., Davies T., Bowman E., 2011. *Quantifying and modeling post-failure sediment yields from laboratory-scale soil erosion and shallow landslide experiments with silty loess*. Geomorphology 129 (2011) 49–58. doi:10.1016/j.geomorph.2011.01.012.
43. Wen-Tzu Lin, Chao-Yuan Lin, Wen-Chieh Chou, 2006. *Assessment of vegetation recovery and soil erosion at landslides caused by a catastrophic earthquake: A case study in Central Taiwan*. Ecological engineering 28 (2006) 79–89. doi:10.1016/j.ecoleng.2006.04.005.

44. Belayneh L., Dewitte O., Gulie G.,, Poesen J., O'Hara D., Kassaye A., Endale T. and Kervyn M., 2022. *Landslides and Gullies Interact as Sources of Lake Sediments in a Rifting Context: Insights from a Highly Degraded Mountain Environment*. Geosciences 2022, 12, 274. https://doi.org/10.3390/geosciences12070274.
45. Mackey, B.H.; Roering, J.J., 2011. *Sediment Yield, Spatial Characteristics, and the Long-Term Evolution of Active Earthflows Determined from Airborne LiDAR and Historical Aerial Photographs*, Eel River, California. Bull. Geol. Soc. Am. 2011, 123, 1560–1576.
46. Poesen, J., 2018. *Soil Erosion in the Anthropocene: Research Needs.* Earth Surf. Processes Landf. 2018, 43, 64–84.
47. Kubwimana, D.; Ait Brahim, L.; Nkurunziza, P.; Dille, A.; Depicker, A.; Nahimana, L.; Abdelouafi, A.; Dewitte, O., 2021. *Characteristics and Distribution of Landslides in the Populated Hillslopes of Bujumbura, Burundi*. Geosciences 2021, 11, 259.
48. Huang F., Chen J., Du Z., Yao C., Huang J., , Jiang Q., Chang Z. and Li S. 2020. *Landslide Susceptibility Prediction Considering Regional Soil Erosion Based on Machine-Learning Models*. ISPRS Int. J. Geo-Inf. 2020, 9, 377; doi:10.3390/ijgi9060377.
49. Kou P., Xu Q., Yunus A., Liu J., Xu Y., Wang C., Li H., Wei Y. & Dong X. 2019. *Landslide-controlled soil erosion rate in the largest tableland on the Loess Plateau, China.* HUMAN AND ECOLOGICAL RISK ASSESSMENT: AN INTERNATIONAL JOURNAL, https://doi.org/10.1080/10807039.2019.1710812.
50. Varnes, D.J., 1978. *Slope Movement Types and Processes*. In: Schuster, R.L. and Krizek, R.J., Eds., Landslides, Analysis and Control, Transportation Research Board, Special Report No. 176, National Academy of Sciences, 11-33.
51. Tavoularis N., Papathanassiou G., Ganas A., Argyrakis P., 2021. *Development of the landslide susceptibility map of Attica Region, Greece based on the method of rock engineering system*. Land journal, https://doi.org/10.3390/land10020148.
52. Wilde M., Günther A., Reichenbach P., Malet J.P. & Hervás J. 2018. *Pan-European landslide susceptibility mapping: ELSUS Version 2.* Journal of Maps. DOI: 10.1080/17445647.2018.1432511. https://doi.org/10.1080/17445647.2018.1432511.
53. Regional Authority of Attica/Directorate of Technical Works, H.S.G.M.E., 2018. *Integrated geological survey for the reduction of flood risk in the wider region of Mandra, Attica – Measures for the prevention and mitigation of flooding phenomena* (Hellenic Survey for Geology and Mineral Exploration (H.S.G.M.E.) – Deliverable II (unpublished).
54. COPERNICUS - Emergency Management Service – Mapping. EMSR257: Flood in Attika, Greece. https://emergency.copernicus.eu/mapping/list-of-components/EMSR257/ALL/EMSR257_01MANDRA.
55. Lekkas E., Voulgaris N., Lozios S. (2017). *Flash Flood in West Attica (Mandra, Nea Peramos) November 15, 2017*. Newsletter of Environmental, Disaster and Crisis Management Strategies Issue No 5, Hellenic Republic National & Kapodistrian University of Athens, https://edcm.edu.gr/images/docs/newsletters/Newsletter201705_Mandra-Floods-eng.pdf.
56. Li, Z.; Fang, H. *Impacts of climate change on water erosion: A review.* Earth Sci. Rev. 2016, 163, 94–117.
57. Labrière, N.; Locatelli, B.; Laumonier, Y.; Freycon, V.; Bernoux, M. *Soil erosion in the humid tropics: A systematic quantitative review*. Agric. Ecosyst. Environ. 2015, 203, 127–139.
58. Li, Y.; Mo, P. *A unified landslide classification system for loess slopes: A critical review*. Geomorphology 2019, 340, 67–83.
59. Blasche P.M, Trustrum N.A., Hicks D.L. Impacts of mass movement erosion on land productivity: A review. Prog. Phys. Geogr. Earth Environ. 2000, 24, 21-52.
60. Ayanlade, A.; Jegede, M.O.; Borisade, P.B. *Geoinformatics in eco-climatic studies*. In Encyclopedia of Information Science and Technology, 3rd ed.; Information Resources Management Association: Hershey, PA, USA, 2014; pp. 3136–3144.
61. Dang, K.; Sassa, K.; Konagai, K.; Karunawardena, A.; Bandara, R.M.S.; Hirota, K.; Tan, Q.; Ha, N.D. *Recent rainfall-induced rapid and long-traveling landslide on 17 May 2016 in Aranayaka, Kagelle District, Sri Lanka*. Landslides 2019, 16, 155–164.
62. Marinos P., Plessas S., Valadaki-Plessa K., 1998. *Thematic maps on the risk assessment of erosion and sediment production in Attica*. Proceedings of the 4th Panhellenic Geographical Conference, pp.584-616, Athens.
63. Glade T., 2003. *Landslide occurrence as a response to land use change: a review of evidence from New Zealand.* CATENA 51(3–4):297–314.

64. Reichenbach P., Galli M., Cardinali M., Guzzetti F., Ardizzone F., 2004. *Geomorphological mapping to assess landslide risk: Concepts, methods and applications in the Umbria region of central Italy*. Landslide Hazard Risk, 429–468.
65. Vianello D., Vagnon F., Bonetto S., Mosca P., 2023. Debris flow susceptibility mapping using the Rock Engineering System (RES) method: a case study. Landslides (2023) 20:735–756, DOI 10.1007/s10346-022-01985-6.
66. Greece Republic, Region of Attica, Directorate for flood protection works, Hydroment Consulting Engineers S.A. - Kritsotakis G. (2021). *Delimitation, settlement and damming of the Soures and Agia Aikaterini streams north of the town of Mandra*. Unpublished technical report.
67. Hudson, J., 1992. *Rock Engineering Systems: Theory and Practice*. Ellis Horwood Limited: Chichester.
68. Hudson, J., 2013. *A Review of Rock Engineering Systems (RES) Applications over the Last 20 Years*; Department of Earth Science and Engineering, Imperial College: London, UK.
69. Tavoularis N., Koumantakis I., Rozos D., Koukis G., 2015. *An implementation of rock engineering system (RES) for ranking the instability potential of slopes in Greek territory. An application in Tsakona area (Peloponnese - Prefecture of Arcadia)*. Bulletin of the Geological Society of Greece vol. XLIX, 38 - 58, 2015. DOI: http://dx.doi.org/10.12681/bgsg.11049.
70. Tavoularis N., Koumantakis I., Rozos D., Koukis G., 2017. *The contribution of landslide susceptibility factors through the use of Rock Engineering System (RES) to the prognosis of slope failures. An application in Panagopoula and Malakasa landslide areas in Greece*. Geotechnical and Geological Engineering journal. DOI 10.1007/s10706-017-0403-9. (http://rdcu.be/yiK7).
71. Brabb, E.; Bonilla, M.G.; Pampeyan, E. *Landslide Susceptibility in San Mateo County, California*. US Geological Survey Miscellaneous Field Studies, Map MF-360, Scale 1:62,500; US Geological Survey: Reston, VA, USA, 1972; reprinted in 1978.
72. Varnes, D.; IAEG Commission on Landslides and Other Mass-Movements. *Landslide Hazard Zonation: A Review of Principles and Practice*; UNESCO Press: Paris, France, 1984; 63p.
73. Gunther A, Reichenbach P., Wilde M., Jurchescu M., Malet J.P., Hervas J (2022). New perspectives on the Europe-wide landslide susceptibility assessment (ELSUS). 2nd EU Soil Observatory Stakeholders Forum, 24-26 June 2022, online.
74. Reichenbach P., Gunther A, Rossi M. (2022). Susceptibility to mass movements at different scales. 2nd EU Soil Observatory Stakeholders Forum, 24-26 June 2022, online.
75. Tavoularis N. (2022). *Soil erosion and landslide susceptibility mapping using Rock Engineering System methodology. The case of Mandra fatal flash flood (2017) in Western Attica, Greece*. 2nd EU Soil Observatory Stakeholders Forum, 24-26 June 2022, online (https://esdac.jrc.ec.europa.eu/euso/presentations-2nd-euso-stakeholders-forum).